



HHS Public Access

Author manuscript

Head Neck. Author manuscript; available in PMC 2020 July 10.

Published in final edited form as:

Head Neck. 2019 June ; 41(6): 1565–1571. doi:10.1002/hed.25604.

Tumor multifocality with vagus nerve involvement as a phenotypic marker of *SDHD* mutation in patients with head and neck paragangliomas: A ¹⁸F-FDOPA PET/CT study

Vincent Amodru, MD¹, Pauline Romanet, PhD², Ugo Scemama, MD³, Marion Montava, MD, PhD⁴, Nicolas Fakhry, MD, PhD⁴, Frédéric Sebag, MD⁵, Frédéric Castinetti, MD, PhD¹, Jean-Pierre Lavieille, MD, PhD², Anderson Loundou, PhD⁶, Arthur Varoquaux, MD, PhD³, Anne Barlier, MD, PhD², Karel Pacak, MD, PhD⁷, David Taïeb, MD, PhD^{8,9}

¹Department of Endocrinology, Conception University Hospital, Aix-Marseille University, Marseille, France ²Laboratory of Molecular Biology, Conception Hospital & CNRS, CRN2M UMR 7286, Aix-Marseille University, Marseille, France ³Department of Radiology, Conception Hospital, Aix-Marseille University, Marseille, France ⁴Department of Otorhinolaryngology-Head and Neck Surgery, Conception Hospital, Aix-Marseille University, Marseille, France ⁵Department of Endocrine Surgery, Conception University Hospital, Aix-Marseille University, Marseille, France ⁶Department of Public Health, EA3279 Self-perceived Health Assessment Research Unit, La Timone University, Aix-Marseille University, Marseille, France ⁷Section on Medical Neuroendocrinology, Eunice Kennedy Shriver National Institute of Child Health & Human Development, National Institutes of Health, Bethesda, Maryland ⁸Department of Nuclear Medicine, La Timone University Hospital, Aix-Marseille University, Marseille, France ⁹European Center for Research in Medical Imaging, Aix-Marseille University, Marseille, France

Abstract

Background—¹⁸F-FDOPA PET/CT was proved to be a highly sensitive imaging method for detecting head and neck paraganglioma (HNPGL). The primary aim of the study was to evaluate the relationship between tumor characteristics and the *SDHx*-mutational status in a large series of patients with HNPGL evaluated by ¹⁸F-FDOPA PET/CT.

Methods—A total of 104 patients with HNPGL (65 sporadic/39 *SDHx*-mutated) were included.

Results—In comparison to *SDHB/SDC/SDHx-negative* cases, patients with *SDHD* were younger at diagnosis and had a higher rate of multifocal, vagal, and carotid paraganglioma. In patients with *SDHD*, vagal paraganglia represented the primary site of tumor origin. Multicentric

Correspondence: David Taïeb, Department of Nuclear Medicine, La Timone University Hospital, European Center for Research in Medical Imaging, Aix-Marseille University, 264 rue Saint-Pierre, 13385 Marseille, France. david.taieb@ap-hm.fr.

AUTHOR CONTRIBUTIONS

All authors provided contributions to study conception, design, acquisition of data or analysis and interpretation of data, drafting the article or revising it critically for important intellectual content, and final approval of the version to be published. Here are the most important contributions of each author:

Study design: Amodru, Varoquaux, Taïeb, Pacak

Data collection: Taïeb, Varoquaux, Amodru, Scemama, Romanet, Sebag, Montava, Barlier, Pacak

Analysis: Taïeb, Varoquaux, Amodru, Pacak

Final responsibility for this article: Taïeb

involvement of the vagus nerve alone or in association with other locations was found to be a typical feature of *SDHD* cases compared to other cases (odds ratio = 59.4).

Conclusion—The present study shows that tumor multifocality within the vagus nerve is a phenotypic marker of *SDHD* mutation. This information is essential in the choice of the therapeutic strategy.

Keywords

diagnostic imaging; genetics; paragangliomas; vagus nerve

1 | INTRODUCTION

Head and neck paragangliomas (HNPGL; often referred to as “glomus tumors”) belong to the family of pheochromocytoma and paraganglioma. They are located in specific areas of the head and neck and more rarely in the anterior or middle mediastinum, in close relationship with the parasympathetic nervous system. Although these tumors have been less investigated than their sympathetic counterparts from an embryological standpoint, it is widely admitted that they derive from the neural crest. HNPGL can be sporadic or can occur as components of paraganglioma (PGL) hereditary syndromes in up to 30%–40% with an increased risk for recurrent behavior and tumor multiplicity.

The molecular genetics era of HNPGL began in 2000, with the description of the first succinate dehydrogenase subunit D (*SDHD*) gene mutation (PGL1 syndrome). Most of *SDHD*-mutation carriers that carry mutation from their father (maternal imprinting) will develop HNPGL that could possibly coexist with sympathetic pheochromocytoma and paraganglioma (PPGL). Of all the known genetic mutations, *SDHD* mutations are currently the leading cause of hereditary HNPGLs, followed by *SDHB* and *SDHC* mutations.^{1–3} Clinical predictors of germline mutations in patients with HNPGL are multiple: family history, previous pheochromocytoma, multiple HNPGL, age > 40 years, and male gender.³ The estimated overall disease penetrance in nonproband *SDHD* mutation carriers (paternally inherited) is at almost twice the penetrance in nonproband *SDHB* mutation carriers.⁴ As hereditary tumors can be millimetric in size, disease penetrance and diagnosis of multifocality patients is widely dependent on the use of high sensitive imaging.

Recently,⁵¹⁸F-FDOPA and ⁶⁸Ga-labeled somatostatin receptor analogs (SSAs) have proved to be the most sensitive positron emission tomography (PET) radiopharmaceuticals in sporadic cases.^{6–8} If not available, SRS using [¹¹¹In]In-DTPA-pentetreotide may be used as an alternative approach, considering the limitations given by spatial resolution of SPECT. ¹⁸F-FDG PET has high sensitivity in the setting of *SDHx*-related HNPGLs but sporadic cases may exhibit low uptake pattern. Based on our longstanding experience in ¹⁸F-FDOPA imaging and literature, false-positive findings in the head and neck region are seen in very rare situations and mainly be related to thyroid tumors of follicular origin,⁹ medullary thyroid carcinoma that can coexist with PPGL in the setting of MEN2 cases and prolactinomas¹⁰ that can be sporadic or related to *SDHx* mutations.

The aim of the present study was to describe ^{18}F -FDOPA findings in a series of patients with HNPGL and evaluate the potential relationships between tumor location and SDH mutational status.

2 | PATIENTS AND METHODS

2.1 | Study design and subjects

This retrospective study was conducted in the department of Nuclear Medicine at La Timone Hospital, Marseille, France. We performed a comprehensive search in our database to identify all patients evaluated by PET/CT from 2007 to 2017 for a presumed HNPGL (based on radiological and functional imaging studies). Among these patients, only those who fulfilled the following criteria were included: (1) final diagnosis of PGL (2) evaluation by ^{18}F -DOPA PET/CT, and (3) genetic testing for at least germline mutations (including large deletions) in the *SDHB*, *SDHD*, and *SDHC* genes. The study was approved by the local ethical committee of Aix- Marseille University. All patients gave informed consent for the use of anonymous personal data extracted from their medical records for research purposes.

2.2 | ^{18}F -DOPA PET/CT imaging protocol

A combined PET/CT scanner was used using Discovery ST or Discovery 710 GE Medical systems. All patients fasted for at least 3 hours. Image acquisition started 45 minutes (20–60 minutes, median 47.5 minutes) after injection of 3.5 Megabecquerels (MBq)/kilogram (kg) of IASODopa (1.8–5 MBq/kg, median 3.4 MBq/kg). The acquisition protocol started with a craniocervical scanning (1 bed position of 10 minutes, headboard, arms along the body), followed by a whole body (WB) acquisition from the top of head to mid thigh (3 minutes/bed position, arms above the head). Each focus of increased extra physiologic radiotracer uptake was recorded and interpreted by an experienced nuclear physician (David Tai'eb). The precise embryological origin of the PPGL was also given.

2.3 | Gold standard

Surgical findings and pathological examination were considered as the gold standard for PGL. In cases where no surgical resection was performed, the diagnosis of PGL and its location was made by the consensus between experienced radiologists and nuclear physicians taking into account all imaging studies (including MRI with angiographic sequences, petrous bone CT, cervico-thoraco-abdominal CT, PET with other radiopharmaceuticals) and follow-up. Vagal paraganglioma (VP) arises within or adjacent to the nerve fibers of the vagus nerve at various levels along its cervico-mediastinal route in the anterior angle formed by the posterolateral common carotid artery and posteromedial internal jugular vein walls. In the upper thorax, The vagus nerve runs in the mediastinum anteriorly to subclavian artery. Combination of ^{18}F -FDOPA tumor uptake (on PET scan) and a typical anatomical location enable diagnosis of VP with a high accuracy. VP are mainly found just below the nodose ganglion. They may extend upward into the skull base through the jugular foramen but tumor volume is mainly located inferiorly in the cervical area. VP can be found at the level of the carotid bifurcation in the retrostyloid parapharyngeal space, splaying anteriorly the internal carotid artery from the internal jugular vein. VP can also rarely be found in the lower neck or the mediastinum in typical locations.

2.4 Genetic analysis and in silico prediction

Genetic analysis was achieved by Sanger sequencing or by targeted Next-Generation Sequencing of blood leukocytes DNA between January 2008 and October 2017 in the laboratory of molecular biology at Conception Hospital. Based on the clinical presentation and the Endocrine Society Clinical Practice Guideline (Lenders et al, JCEM 2014), the genetic testing of the *SDHB* (NM_003000.2), *SDHC* (NM_003001.3), and *SDHD* (NM_003002.3) genes was performed for all the index cases after that their informed consents were obtained. The full coding sequences and exon-intron junctions of these genes were analyzed. The variant changes were named using the HGVS nomenclature. The *SDHB*/*SDHC*/*SDHD* sequence variants were classified as pathogenic/likely pathogenic/variants of uncertain significance (VUS)/likely benign/benign according the ACMG-AMP Standards and guidelines for the interpretation of sequence variants.¹¹ For unknown variants, silico analysis was performed using Alamut Visual (Interactive Biosoftware, Rouen, France). The splicing impact of the variations was evaluated using Human Splicing Finder 3.1 (MMG, Marseille, France). The bibliographic references of the different sequence variants were found using the Human Gene Mutation Database (HGMD).

2.5 Statistical analysis

Statistical analysis was performed using IBM SPSS Statistics version 20 (IBM SPSS Inc., Chicago, Illinois). Continuous variables are expressed as means \pm SD and categorical variables are reported as count and percentages. Logistic regression model was used to find variables that were found to be associated with *SDHD* mutation status. Odds ratios were expressed with 95% confidence intervals. All the tests were two-sided. The statistical significance was defined as $P < .05$.³ *SDHD*, single VP in another patient with *SDHD* and a single carotid body paraganglioma (CBP) in the latter patient with *SDHC*. None of the nonprobans cases received any specific prior therapy for their HNPGL.

The use of pathogenic variants prediction tools allowed us to reclassify two variants as likely benign variants (one of them initially classified as a *SDHB* mutation and the other one initially classified as a Von Hippel-Lindau (VHL) mutation). Thus, these variants were considered as sporadic cases. The mean age at diagnosis was 58.1 ± 15 years and 66.33% of patients with HNPGL were female.

3.2 Tumor locations across genotypes, with special emphasis on VP

The percentages of multifocality in patients with *SDHB*, *SDHD*, *SDHC*, and sporadic HNPGL were 0%, 78.2%, 25%, and 10.7%, respectively (Table 1). Regarding the PGL associated with the vagus nerve (VP), they were diagnosed in 0% of the *SDHB* mutation carriers, 86.9% (n = 20) of the *SDHD* mutation carriers, 12.5% (n = 1) of the *SDHC* mutation carriers, and 23.1% (n = 15) of the sporadic cases (Table 1, Figure 1). 69.5% (n = 16) of *SDHD* mutations carrier patients had multifocal VP, whereas there were only 0%, 12.5% (n = 1), and 3.1% (n = 2) in *SDHB*, *SDHC*, and sporadic cases, respectively (Table 2). VP in *SDHD* typically occurs at the level of the nodose ganglion with additional tumors within the vagus nerve trunk (Table 2).

3.3 Genotype-phenotype correlations in patients with *SDHD*

Eleven different variants were identified in *SDHD* mutation carriers. Among them, two nucleotidic variants were over represented: c.169+5G>A and c.129G>A, both located in exon 2. Mediastinal VP was only detected in patients with *SDHD*. Focusing on the c.129G>A variant, it appears clear that this genotype is more likely to express a phenotype with a mediastinal vagus location (OR = 7.14; $P = 5 \times 10^{-21}$). Indeed, among the 104 patients with HNPG, 6 out of the 7 patients with a mediastinal vagus location are patients with *SDHD* having a c.129G>A variant (Table 3). The two most represented variants: c.169+5G>A ($n = 6$) and c.129G>A ($n = 6$) have previously been reported in the literature (Cascon, et al.¹³; Timmers, et al.¹⁴). The c.169+5G>A variant has been described as potentially metastatic. Indeed, in our study, one out of the 6 c.169+5G>A variants (the only one among *SDHD* variants) presented distant metastasis at diagnosis, (Table 1) confirming that we should consider this variant as a potentially malignant condition. The c.129G>A variant was described once in the literature and presented a para-aortic localization; these results are in accordance with our findings. Four variants have never been reported in the literature: c.1A>G, c.446–449delinsA, c.64C>T, and c.433–438del (Table 3). Ultimately, among the three nonsense mutations coding for truncated proteins: c.129G>A ($n = 6$), c.325C>T ($n = 3$), and c.64C>T ($n = 1$); 100% of them were VP with multifocality (Table 3).

4 | DISCUSSION

To the best of our knowledge, this is the largest study that describes the locations of HNPG across genotypes based on modern imaging, including 18F-DOPA PET/CT. Although our series was biased by the recruitment process from the department of Nuclear Medicine, the prevalence of *SDHB/C/D* in our population (37.5%) was in accordance with the literature. The unique missing location was tympanic PGL (ie, Fisch classes A and B). As these tumors are almost always sporadic and often cured by surgical resection, they are usually not evaluated by functional imaging in our institution.

The principal conclusions that can be drawn from this study include: (1) confirmation that HNPG mainly occur in the context of sporadic and *SDHD* cases, (2) vagal location is the most common primary site of HNPG in *SDHD* cases, and (3) presence of tumor multifocality with vagus nerve involvement should be considered as an important phenotypic marker of *SDHD*-related disease.

Several studies have shown that *SDHD* was the leading cause of hereditary HNPG and this finding was recently illustrated in a large study of 876 patients with *SDHB/C/D* that reported genotype-phenotype correlations as well as penetrance disease across genotypes.⁴ However, detailed information regarding the locations of HNPGs are lacking in most series. A large prospective study that evaluated 259 *SDHx*-mutations carriers with octreoscan and magnetic resonance angiography showed that VP mainly occurred in presence of *SDHD*-mutation, 33 of 37 and 10 of 10 being detected in *SDHD* index cases and relatives, respectively.¹⁷ In another study that evaluated 72 patients with *SDHx* by contrast-enhanced CT, 23 of 27 VP were observed in patients with *SDHD*.¹⁸ In both series, carotid body PGL was the most common location in patients with *SDHD*. In our series, we found that the vagus nerve paraganglia represented the most common location of the primary tumor in *SDHD* cases.

This was probably due to the use of high sensitive PET/CT imaging. The continuing evolution of anatomical imaging and functional imaging has drastically increased the penetrance of HNPGL and prevalence of VP that could be millimetric in size, especially in the setting of hereditary PGL syndromes. In two prospective studies,^{7,8} ⁶⁸Ga- DOTATATE PET/CT was found to be slightly superior (not statistically) to F-FDOPA PET/CT in the detection of primary HNPGL in patients with *SDHx*, mainly due to the combination of a highly elevated tumor-background ⁶⁸Ga- DOTATATE uptake ratio and the catecholaminergic differentiation pattern of *SDHx*-related PGL. However, ⁵F-FDOPA PET/CT has excellent value in the location of HNPGL. The knowledge of genetic status and tumor multifocality has important clinical implications and is essential in the decision of the therapeutic strategy. In fact, surgical management of HNPGL can be challenging due to complex anatomy and nearby critical structures. Although subtotal surgical approaches have been developed to limit cranial nerve morbidity, surgical resection of HNPGL may lead to severe, permanent surgery-induced injuries (ie, dysphagia, chronic aspiration, vocal cord paralysis) and may compromise subsequent operations. Radiosurgery and conventional radiotherapy can control tumoral evolution but not without risk of cranial nerve morbidity. The present study shows that tumor multifocality with vagus nerve involvement is an important phenotypic marker of *SDHD*-related disease. As surgical management of HNPGL can be followed by secondarily neurological injuries, the presence of contralateral PGL especially VP may compromise further surgical and radiosurgical intervention. Surgical resection of VP almost always leads to the sacrifice of the vagus nerve, and sometimes palsy of other adjacent cranial nerves.¹⁹ It is important to recall that bilateral neurological injuries affect respiration, deglutition, and phonation and are associated with chronic complications and vital risks. Therefore, the impact of detecting VP at the primary workup is of a major clinical importance, especially in patients with tumor multifocality with bilateral VP or VP associated with contralateral CBP or jugular paraganglioma (JP). In patients with HNPGL, a conservative management should be proposed to prevent any neurological injuries until genetic testing and functional imaging results.

Interestingly, patients with *SDHB* and *SDHC* are unlikely to have multifocal disease, even when evaluated ⁵F-FDOPA PET/CT. Therefore, these patients should probably be treated as sporadic cases.

The optimal follow-up algorithm has not yet been validated in nonproband *SDHx*-PPGLs but most likely requires a more frequent and complete imaging workup than for their sporadic counterparts. The aim is to detect tumors at early stages of development, thereby minimizing tumor extension, and cranial nerve impairment as for example, published for *SDHD*-related HNPGLs,²⁰ facilitating curative treatment, and potentially reducing the occurrence of local and distant metastatic spread, especially in more aggressive genotypes (eg, *SDHB*). At initial staging, the use of PET imaging should provide an adequate sensitivity and specificity at WB scale with limited radiation exposure. Based on clinical studies, ⁶⁸Ga-DOTA-SSAs PET should be prioritized if available over ¹⁸F-FDOPA PET, although its indication has not been specifically studied in this setting nonproband *SDHx* cases. In absence of PPGL, follow-up should include annual biochemical screening, especially plasma methoxytyramine and MRI at regular time intervals.²¹ MRI may be done every 1–2 years for *SDHD*-related HNPGLs, but for *SDHB* ones, we would recommend to

consider this imaging study to be done every year. For *SDHA* and *SDHC*HNPGLs, data are limited but perhaps these patients can follow the same guidelines as for patients with *SDHD*.

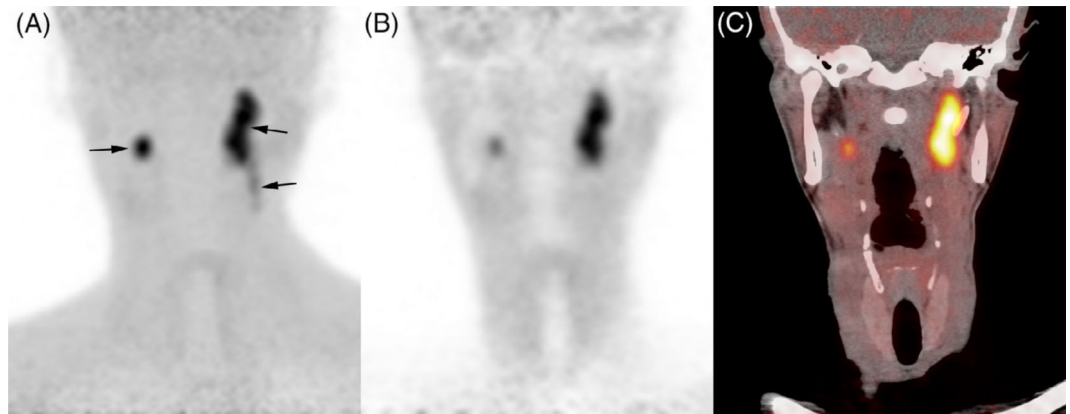
VPs arise from neural-crest derived endocrine cells associated with the vagus nerve. The so-called vagal body paraganglia has been originally described in birds by Muratori in 1932²² and in humans by White in 1935.²³ In fact, it is constituted by an average of 6–7 separate collections of paraganglia, mainly located at or just below (2.0 cm) the level of nodose ganglion (ie, inferior ganglion), within the nerve or ganglion itself.¹ The nodose ganglion contains cell bodies of the sensory neurons that transmits visceral stimuli (taste buds, heart, lungs, and other visceral organs) to the nucleus of the solitary tract. Additional paraganglionic cells clusters could be found in distal portions of the vagus nerve. Despite similar architectural and cytochemical features between vagal body paraganglia and carotid bodies, its chemoreceptor role is still unclear despite possible observation of chief cell hyperplasia during chronic hypoxemia.⁵

Stout identified the first paraganglioma of the vagus nerve,²⁴ and Birrell proposed the term vagal body tumor in 1953.²⁵ During the past decades, several case series have been reported VP with possible multifocality with other PGL and malignant potential. Its possible familial occurrence has been formally recognized after it has been made for carotid and jugular PGL.^{26,27} Although, HNPGL can be related to *SDH* mutations, they are often sporadic. In these cases, mechanisms involved in tumorigenesis are still to be established. In *SDHx*-related PGL, *SDH* acts as a tumor suppressor in the paraganglionic system. Tumorigenesis requires a second hit that leads to *SDH* deficiency.

REFERENCES

1. Baysal BE, Willett-Brozick JE, Lawrence EC, et al. Prevalence of *SDHB*, *SDHC*, and *SDHD* germline mutations in clinic patients with head and neck paragangliomas. *J Med Genet*. 2002;39(3):178–183. [PubMed: 11897817]
2. Piccini V, Rapizzi E, Bacca A, et al. Head and neck paragangliomas: genetic spectrum and clinical variability in 79 consecutive patients. *Endocr Relat Cancer*. 2012;19(2):149–155. [PubMed: 22241717]
3. Neumann HP, Erlic Z, Boedeker CC, et al. Clinical predictors for germline mutations in head and neck paraganglioma patients: cost reduction strategy in genetic diagnostic process as fall-out. *Cancer Res*. 2009;69(8):3650–3656. [PubMed: 19351833]
4. Andrews KA, Ascher DB, Pires DEV, et al. Tumour risks and genotype- phenotype correlations associated with germline variants in succinate dehydrogenase subunit genes *SDHB*, *SDHC* and *SDHD*. *J Med Genet*. 2018; 55(6):384–394. [PubMed: 29386252]
5. Lack EE. Hyperplasia of vagal and carotid body paraganglia in patients with chronic hypoxemia. *Am J Pathol*. 1978;91(3):497–516. [PubMed: 655261]
6. Taieb D, Pacak K. New insights into the nuclear imaging phenotypes of cluster 1 pheochromocytoma and paraganglioma. *Trends Endocrinol Metab*. 2017;28(11):807–817. [PubMed: 28867159]
7. Archier A, Varoquaux A, Garrigue P, et al. Prospective comparison of (68) Ga-DOTATATE and (18)F-FDOPA PET/CT in patients with various pheochromocytomas and paragangliomas with emphasis on sporadic cases. *Eur J Nucl Med Mol Imaging*. 2016;43(7):1248–1257. [PubMed: 26637204]
8. Janssen I, Chen CC, Taieb D, et al. 68Ga-DOTATATE PET/CT in the localization of head and neck paragangliomas compared with other functional imaging modalities and CT/MRI. *J Nucl Med*. 2016;57(2):186–191. [PubMed: 26564322]

9. Pauleau G, Palazzo FF, Essamet W, Sebag F, Taieb D. Hurthle cell neoplasms: a new differential diagnosis for 18F-FDOPA-avid thyroid nodules? *J Clin Endocrinol Metab.* 2013;98(3):865–866. [PubMed: 23337720]
10. Ginet M, Cuny T, Schmitt E, Marie PY, Verger A. 18F-FDOPA PET imaging in prolactinoma. *Clin Nucl Med.* 2017;42(8):e383–e384. [PubMed: 28590300]
11. Group NGSiPS Toledo RA, Burnichon N, et al. Consensus Statement on next-generation-sequencing-based diagnostic testing of hereditary pheochromocytomas and paragangliomas. *Nat Rev Endocrinol.* 2017;13(4):233–247. [PubMed: 27857127]
12. Lima J, Feijao T, Ferreira da Silva A, et al. High frequency of germline succinate dehydrogenase mutations in sporadic cervical paragangliomas in northern Spain: mitochondrial succinate dehydrogenase structure-function relationships and clinical-pathological correlations. *J Clin Endocrinol Metab.* 2007;92(12):4853–4864. [PubMed: 17848412]
13. Cascon A, Ruiz-Llorente S, Cebrian A, et al. Identification of novel SDHD mutations in patients with pheochromocytoma and/or paraganglioma. *Eur J Hum Genet.* 2002;10(8):457–461. [PubMed: 12111639]
14. Timmers HJ, Pacak K, Bertherat J, et al. Mutations associated with succinate dehydrogenase D-related malignant paragangliomas. *Clin Endocrinol (Oxf).* 2008;68(4):561–566. [PubMed: 17973943]
15. Baysal BE, Ferrell RE, Willett-Brozick JE, et al. Mutations in SDHD, a mitochondrial complex II gene, in hereditary paraganglioma. *Science.* 2000; 287(5454):848–851. [PubMed: 10657297]
16. Burnichon N, Rohmer V, Amar L, et al. The succinate dehydrogenase genetic testing in a large prospective series of patients with paragangliomas. *J Clin Endocrinol Metab.* 2009;94(8):2817–2827. [PubMed: 19454582]
17. Gimenez-Roqueplo AP, Caumont-Prim A, Houzard C, et al. Imaging workup for screening of paraganglioma and pheochromocytoma in SDHx mutation carriers: a multicenter prospective study from the PGL.EVA investigators. *J Clin Endocrinol Metab.* 2013;98(1):E162–E173. [PubMed: 23162105]
18. Michalowska I, Lewczuk A, Cwikla J, et al. Evaluation of head and neck Paragangliomas by computed tomography in patients with Pheochromocytoma- Paraganglioma syndromes. *Pol J Radiol* 2016;81:510–518. [PubMed: 27867439]
19. Suarez C, Rodrigo JP, Bodeker CC, et al. Jugular and vagal paragangliomas: systematic study of management with surgery and radiotherapy. *Head Neck.* 2013;35(8):1195–1204. [PubMed: 22422597]
20. Heesterman BL, de Pont LMH, van der Mey AG, et al. Clinical progression and metachronous paragangliomas in a large cohort of SDHD germline variant carriers. *Eur J Hum Genet.* 2018;26:1339–1347. [PubMed: 29777207]
21. Daniel E, Jones R, Bull M, Newell-Price J. Rapid-sequence MRI for long-term surveillance for paraganglioma and pheochromocytoma in patients with succinate dehydrogenase mutations. *Eur J Endocrinol.* 2016;175(6): 561–570. [PubMed: 27634942]
22. Muratori G Contributo all'innervazione des tessuto paragangliare annesso al sistema del vago (glomus carotico, paragangli extravagali ed intravagali) e all' innervazione del seno carotideo. *Anat Anz* 1932;75:115–123.
23. White EG. Die Struktur des Glomus caroticum, seine Pathologie und Physiologie und seine Beziehung zum Nervensystem. *Beitr Pathol Anat Allgemienen Pathol.* 1935;96:177–227.
24. Stout AP. The malignant tumors of the peripheral nerves. *Am J Cancer.* 1935;25:1–36.
25. Birrell JH. The vagal body and its tumour. *Aust N Z J Surg.* 1953;23(1): 48–54. [PubMed: 13081537]
26. Linn HJ, Proctor B. Tumor of the ganglion nodosum of the vagus nerve. *Laryngoscope.* 1956;66:1577–1581. [PubMed: 13386301]
27. Kahn LB. Vagal body tumor (nonchromaffin paraganglioma, chemodectoma, and carotid body-like tumor) with cervical node metastasis and familial association: ultrastructural study and review. *Cancer.* 1976;38(6): 2367–2377. [PubMed: 187317]

**FIGURE 1.**

Bilateral vagus nerve PGL in a patient with *SDHD*. ^{18}F -FDOPA PET (maximal intensity projection), coronal ^{18}F -FDOPA PET.

A, Craniocervical ^{18}F -FDOPA PET image (maximal intensity projection) showing bilateral VP (arrows); B, Correction-attenuation coronal ^{18}F -FDOPA PET image; C, Coronal ^{18}F -FDOPA PET/CT fusion image

TABLE 1

Patient's and tumors' characteristics across genotypes

| Gene mutated | SDHD (n = 23, 22.1%) | SDHB (n = 8, 7.7%) | SDHC (n = 8, 7.7%) | Negative genetic testing (n = 65, 62.5%) | SDHD vs other | | P |
|----------------------|----------------------|--------------------|--------------------|--|---------------|------------|-------|
| | | | | | OR | 95% CI | |
| Age | 45.1 ± 13.1 | 55.6 ± 13.7 | 53.2 ± 16.4 | 63.4 ± 12.6 | 0.9 | 0.88–0.96 | <.001 |
| Female, n (%) | 11 (47.8) | 2 (25) | 6 (75) | 50 (76.9) | 0.4 | 0.14–0.94 | .033 |
| Multifocality, n (%) | 18 (78.2) | 0 (0) | 2 (25) | 7 (10.7) | 28.8 | 8.6–96.49 | <.001 |
| VP, n (%) | 20 (86.9) | 0 (0) | 1 (12.5) | 15 (23.1) | 27.1 | 7.16–102.5 | <.001 |
| CBP, n (%) | 14 (60.8) | 2 (25) | 6 (75) | 18 (27.7) | 3.3 | 1.26–8.58 | .012 |
| JP, n (%) | 10 (43.4) | 6 (75) | 3 (37.5) | 34 (52.3) | 0.7 | 0.27–1.73 | .416 |
| Metastatic, n (%) | 1 (4.3) | 1 (12.5) | 0 (0) | 1 (1.5) | 1.8 | 0.16–20.73 | .531 |

Bold values indicate statistical significance ($P < .05$).

TABLE 2

Relationship between vagus nerve involvement and patient's genotype

| Gene mutated | SDHD (n = 23, 22.1%) | SDHB (n = 8, 7.7%) | SDHC (n = 8, 7.7%) | SDHD vs others | | |
|--|----------------------|--------------------|--------------------|----------------|------------|-------|
| | | | | OR | 95% CI | P |
| Number of patients with VP (%) | 20 (86.9) | 0 (0) | 1 (12.5) | 27.1 | 7.16–102.5 | <.001 |
| Number of patients with multiple VP (%) | 16 (69.5) | 0 (0) | 1 (12.5) | 59.4 | 13.8–254.7 | <.001 |
| Single VP without additional PPGL, number of patients: n (%) | 4 (17.3) | 0 (0) | 0 (0) | 1.1 | 0.32–3.77 | .999 |
| Single VP with parasympathetic PGL only, n (%) | 0 (0) | 0 (0) | 1 (12.5) | NA | NA | NA |
| Single VP with parasympathetic PGL and sympathetic PPGL, n (%) | 0 (0) | 0 (0) | 0 (0) | NA | NA | NA |
| Multiple VP without additional PPGL, n (%) | 1 (4.34) | 0 (0) | 0 (0) | NA | NA | NA |
| Multiple VP with parasympathetic PGL only n (%) | 9 (39.1) | 0 (0) | 0 (0) | 6.8 | 4.2–11.0 | <.001 |
| Multiple VP with parasympathetic PGL and sympathetic PPGL, n (%) | 6 (26.1) | 0 (0) | 0 (0) | 5.8 | 3.74–8.88 | <.001 |
| Nodose VP only, n (%) | 9 (45) | 0 (0) | 1 (100) | 1.05 | 0.2–3.9 | 1 |
| Nodose + trunk VP, n (%) | 10 (50) | 0 (0) | 0 (0) | 7 | 1.2–39 | .03 |
| Trunk VP only, n (%) | 1 (5) | 0 (0) | 0 (0) | 0.06 | 0.007–0.6 | .01 |

Bold values indicate statistical significance ($P < .05$).

TABLE 3

Relationship between genotype and phenotype in patients with *SDHD*

| Exon | 1 | 2 | 2 | 2 | 3 | 3 | 3 | 3 | 4 | 4 | 4 |
|-----------------------------|--------------|---------------------------|--------------|-----------------------------|------------------------------|-----------------------------|-----------------------------|--------------------------------|--------------------------------|--------------------|--------------------------|
| Nucleotide change | c.11A>G | c.56G>T | c.64C>T | c.129G>A | c.169+5G>A | c.242C>T | c.274G>T | c.305A>C | c.325C>T | c.433_438del | c.446_449delinsA |
| Peptidic change | p.? | p.Arg17Leu | p.Arg22* | p.Trp43* | p.? | p.Pro81Leu | p.Asp92.Tyr | p.His102Pro | p.Gln109* | p.His145_Asp146del | p.Ile149_Cys150delinsAsn |
| Effect | Start loss | False-sense | Non-sense | Non-sense | Splice | False-sense | False-sense | False-sense | Non-sense | In frame deletion | In frame deletion |
| Interpretation | P | LP | P | P | P | P | P | LP | P | LP | LP |
| Affected patients | 1 | 1 | 6 | 6 | 6 | 1 | 1 | 1 | 3 | 1 | 1 |
| Unifocal | 0 | 0 | 1 | 1 | 2 | 1 | 0 | 0 | 0 | 1 | 0 |
| Multifocality | 1 | 1 | 5 | 4 | 4 | 0 | 1 | 1 | 3 | 0 | 1 |
| Metastatic | 0 | 0 | 0 | 1 | 1 | 0 | 0 | 0 | 0 | 0 | 0 |
| VP (cervical only) | 1 | 1 | 1 | 0 | 3 | 1 | 1 | 0 | 3 | 1 | 1 |
| VP (mediastinal only) | 0 | 0 | 1 | 0 | 0 | 0 | 0 | 1 | 0 | 0 | 0 |
| VP (cervical + mediastinal) | 0 | 0 | 5 | 0 | 0 | 0 | 0 | 0 | 0 | 0 | 0 |
| Extra vagal PGL only | 0 | 0 | 0 | 0 | 3 | 0 | 0 | 0 | 0 | 0 | 0 |
| Reference | Not reported | Lima et al. ¹² | Not reported | Cascon et al. ¹³ | Timmers et al. ¹⁴ | Baysal et al. ¹⁵ | Baysal et al. ¹⁵ | Burnichon et al. ¹⁶ | Burnichon et al. ¹⁶ | Not reported | Not reported |

* = mutations that lead to the coding of a STOP codon.